Lawrence Berkeley National Laboratory
Recent Work

Title
Defect Formation in Epitaxial Crystal Growth

Permalink
https://escholarship.org/uc/item/5pm502k4

Authors
Washburn, J.
Kvam, E.P.
Liliental-Weber, Z.

Publication Date
1990-05-01

eScholarship.org Powered by the California Digital Library
University of California

UC404

LBL-29038
Preprint

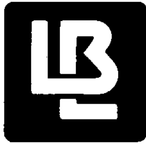

Lawrence Berkeley Laboratory

UNIVERSITY OF CALIFORNIA

Materials & Chemical Sciences Division

Submitted to Journal of Electronic Materials

Defect Formation in Epitaxial Crystal Growth

J. Washburn, E.P. Kvam, and Z. Liliental-Weber

May 1990

For Reference

Not to be taken from this room

LBL-29038
Copy 1
Bldg. 50 Library.

Prepared for the U.S. Department of Energy under Contract Number DE-AC03-76SF00098.

DISCLAIMER

This document was prepared as an account of work sponsored by the United States Government. While this document is believed to contain correct information, neither the United States Government nor any agency thereof, nor the Regents of the University of California, nor any of their employees, makes any warranty, express or implied, or assumes any legal responsibility for the accuracy, completeness, or usefulness of any information, apparatus, product, or process disclosed, or represents that its use would not infringe privately owned rights. Reference herein to any specific commercial product, process, or service by its trade name, trademark, manufacturer, or otherwise, does not necessarily constitute or imply its endorsement, recommendation, or favoring by the United States Government or any agency thereof, or the Regents of the University of California. The views and opinions of authors expressed herein do not necessarily state or reflect those of the United States Government or any agency thereof or the Regents of the University of California.

LBL-29038

DEFECT FORMATION IN EPITAXIAL CRYSTAL GROWTH

J. Washburn, E.P. Kvam, and Z. Liliental-Weber

Materials & Chemical Sciences Division
Lawrence Berkeley Laboratory
University of California, Berkeley, CA. 94720

Submitted to Journal of Electronic Materials

This work was supported by the Director, Office of Energy Research, Office of Basic Energy Sciences, Material Sciences Division of the U.S. Department of Energy under Contract No. DE-AC03-76SF00098.

Defect Formation in Epitaxial Crystal Growth

Jack Washburn, Eric P. Kvam, and Zuzanna Lilliental-Weber
Materials and Chemical Sciences Division,
Lawrence Berkeley Laboratory, Berkeley, CA 94720

Factors affecting the nucleation and propagation of dislocations, stacking faults, microtwins, and inversion domain boundaries in epitaxially grown semiconductor layers are reviewed, with examples for heteroepitaxial MBE-grown layers on substrates having varying degrees of mismatch or different crystal symmetry. Mechanisms for generation of defects at the heterointerface and in the epilayer are discussed. For epilayers with bulk mismatch from 0 to 4%, methods for reducing defect density in the epitaxial layer are considered. Examples of structural details in the epilayers and at heterointerfaces, particularly those which may be revealed by transmission electron microscopy, are given.

Defect Formation in Epitaxial Crystal Growth

Jack Washburn, Eric P. Kvam, and Zuzanna Lilliental-Weber

Abstract

Factors affecting the nucleation and propagation of dislocations, stacking faults, microtwins, and inversion domain boundaries in epitaxially grown semiconductor layers are reviewed, with examples for heteroepitaxial MBE-grown layers on substrates having varying degrees of mismatch or different crystal symmetry. Mechanisms for generation of defects at the heterointerface and in the epilayer are discussed. For epilayers with bulk mismatch from 0 to 4%, methods for reducing defect density in the epitaxial layer are considered. Examples of structural details in the epilayers and at heterointerfaces, particularly those which may be revealed by transmission electron microscopy, are given.

Introduction

Epitaxial growth is an extremely wide-spread phenomenon in crystalline materials. In the broadest sense, all crystal growth is epitaxial, in that each successive layer of any crystal grows on the previously grown "substrate" crystal. More commonly, the term epitaxial is used to describe crystal growth that continues through an interface where there is a change in crystal structure and/or composition in such a way that a special orientation relationship is preserved across the interface. When the surface of a substrate crystral is truly clean of contaminants, epitaxial growth is the rule rather than the exception. This is the case even for widely different crystal structure, bonding type, or lattice parameter variations across the interface. There is usually a special relative orientation relationship, e.g. which maximizes atomic alignment across the interface, such that growth of that particular orientation is preferred. This tendency is a technologically useful phenomenon in that, on a single crystal substrate, it often permits the growth of a single crystal thin film of

a different material. This is of vast practical interest for semiconductor technology, for the new high-Tc superconducting thin films, and for devices based on strained or ordered layer superlattices.

Considerable research activity has developed on expanding applications of hetero-epitaxial films, particularly within the past ten years, with the development of MBE and other sophisticated growth techniques. The aim of this research has been to understand the origin and characteristics of the defects in epitaxially grown layers well enough to avoid their formation, or to devise ways to reduce their densities after film growth, so as to achieve nearly perfect, device-quality heteroepitaxial layers.

Origins of Defects

Transmission electron microscopy (TEM) studies in cross section and plan view have shown that the defects in epitaxial layers have a number of different origins:

1) Linear or areal defects in the substrate are extended during growth into the epilayer. The density of these defects in the new material is then at least equal to that of the substrate. The new heterolayer can thus be of no higher quality than its substrate, at least initially.

2) New defects are introduced directly at the epilayer interface with the substrate. This is particularly true if removal of oxide or other contaminants from the surface of the substrate has not been complete; an example is shown in Figure 1. Even for a perfectly clean substrate, surface topography (such as steps) can induce defects when there is a loss of symmetry in the epilayer relative to the substrate, such as inversion boundaries in GaAs/Si(100), as seen in Figure 2. Similarly, when the symmetry of the orientation relation is greater than that of the epilayer material, the epilayer may contain twins or grain boundaries.

3) As is the case for any crystal growth, simple growth mistakes can, in certain circumstances, lead to microtwins, stacking faults, inclusions of impurities, or even to polycrystalline or amorphous growth.

4) Clustering of excess point defects (vacancies, interstitials, impurities) during growth, or on cooling after growth, can lead to formation of dislocation loops or more complex defects.

5) Stresses induced to accomodate coherence of mismatched lattice dimensions across the heterointerface can result in plastic deformation of the epilayer in order to generate the array of misfit dislocations at the heterointerface required for minimum free energy of the system. In addition to misfit dislocations lying in the interface, this plastic deformation usually leaves dislocation segments which thread through the epilayer. For large misfits, such as the 4% mismatch between Si and GaAs, the density of threading dislocations can be very high, as illustrated in Figure 3.

Stacking faults, microtwins, point defect clusters, and precipitates can be eliminated for many cases by use of high quality substrates, avoidance of contamination or adverse surface geometries, and careful control of growth conditions, or by post-growth annealing. However, the introduction of dislocations through strain-induced plastic deformation cannot be avoided for thick mismatched films.

Mismatched Epitaxy

The lattice mismatch between a heteroepitaxial film and its substrate can be accomodated entirely by elastic strains (Figure 4), or can be partially relaxed by introduction of a grid of dislacations at the interface (Figures 5 & 6). The introduction of misfit dislocations becomes energetically favorable only after the film exceeds a critical thickness, h_c, which decreases as the lattice mismatch increases[1] . Figure 7 shows a plot of this critical thickness as a function of lattice mismatch. Below the curve, misfit

dislocations would increase the free energy of the system and will not be formed, while above this curve they may be introduced.

In practice, there are two different curves for h_c, one representing the absolute thermodynamic limit (developed by van der Merwe)[2], and the second (developed by Matthews, et alia)[1,3,4] representing the absolute kinetic limit. In essence, the latter incorporates the consideration that dislocations must have some introduction mechanism, and thus describes a thremodynamically metastable (though kinetically stable) final state.

A very large number of experimental observations and theoretical calculations have been devoted to understanding the mechanisms by which misfit dislocations are generated, and how these mechanisms relate to the density of dislocations which thread through the epilayer. Perhaps the most obvious mechanism is that dislocations already present, on a glide plane and with a component of the misfit stress acting in the direction of the Burgers vector, will glide through the epilayer so as to be extended into the interface (Figure 8). However, for substrates that are almost dislocation-free (e.g. semiconductor-grade Si), there are far too few such dislocations to make any significant contribution.

The $Si_{1-x}Ge_x$/Si system has been widely used to study systematically the effect of lattice mismatch and dislocation introduction, because other effects at the interface are almost wholly negated -- there is little bulk diffusion at growth temperatures, essentially no charge transfer or ordering/segregation effects, etc. -- and the lattice mismatch may be varied continuously from 0 to 0.042 over the range $0 \leq x \leq 1$.

Extensive etch pit[5] and TEM[6-10] observations have shown that for misfit strains below about 0.018, new dislocation loops are nucleated primarily at small inclusions or other stress-concentrating defects that have been grown into the epilayer. They frequently spread out from these centers on several possible glide planes. Back stresses from the first loops emitted can also lead to cross slip of subsequent loops. In semiconductor materials, particularly Si, the Peierls-Nabarro stress is extremely high, so that glide motion of the dislocations must be thermally activated. Therefore, at typical growth temperatures

(~500°C), dislocation glide is slow even though the misfit stress can be very high. The result is that numerous half-loops spread slowly out from these centers at a velocity which is a function of the excess stress (the misfit stress minus the effective back stresses due to dislocation line tension and other dislocations). The net force acting on the dislocations increases with film thickness, h, because the net force on the moving segment is integrated over the threading length ($h \cdot \sigma_{eff}$). Dodson and Tsao have suggested that the dependence of dislocation velocity on thickness explains the observation that little detectable relaxation of misfit strain is observed until a thickness appreciably greater than h_c is reached[11-13].

In-situ annealing experiments carried out in the TEM on films grown in this regime showed that films grown apparently dislocation-free but above the curve were indeed only metastable[14]. Upon annealing at temperatures at or above the growth temperature, dislocations did gradually appear and their velocities could be measured. These data were used to develop phenomenological models of the dislocation motion which took place during introduction of misfit dislocations into the heterointerfaces of these mismatched layers, as a function of thickness, mismatch, time, and temperature. Other very sensitive techniques have also been applied to the observation of dislocation introduction (PL imaging, electrical measurements, x-ray topography), showing that some misfit dislocations were present, albeit at very low densities, in films initially believed to be metastable. Some reports of metastable, "dislocation-free" film growth appear in the literature for points beyond the Matthews curve, but they are probably only "dislocation-free" to the sensitivity of the experimental techniques utilized[15].

The strain concentrator in reference 5 was probably an oxide particle; the same group has done work showing other sources' effects as well[16] (e.g. scratches). There are other possible defects, and the typical defect densities measured by etching studies give a post-growth density which is often an order of magnitude above the initial substrate density, even for stable films (below the Matthews line) in which no misfit dislocation introduction is energetically allowed. Although not necessarily a general phenomenon, one

such defect has been identified, and shown to be a source for multiple dislocations[17,18] (diamond defect). This defect, or similar others, would be sufficient to explain the dislocation numbers observed.

The diamond defect was shown to be a faulted, highly crystallographic loop with a {111} habit and inclined <110> edges. The bounding dislocation (and fault vector) were of the type 1/6<411>. This bounding dislocation could dissociate into two different combinations of a sessile 1/6<211> plus glissile 1/2<110> dislocations, with different dissociations available at the two bounding line orientations, and with two different glide planes available to each of the glissile 1/2<110> dislocations. The glissile dislocation segment, if considered by itself, is easily recognizable as a classical Frank-Read source configuration. That is, it could, under the influence of the misfit stresses, produce a free glissile loop (which would become a half-loop on reaching the surface, and leave an interfacial misfit dislocation at the heterointerface), with the initial dislocation configuration reforming to operate again. The crystallography of the diamond defect allows, in principle, the production of six of the eight possible 60° type misfit dislocation Burgers vector/line direction combinations, and defects were in fact identified which had operated to produce at least three of these.

It is clear from the etch pit observations that when a number of half-loops have been emitted from a heterogeneous source, and glide out along the four glide planes which intersect the source, some of them cross slip so as to form new half-loops on the cross slip planes. Cross slip of a screw segment of a half-loop becomes probable when a number of preceding loops on the same glide plane impede further glide to and along the interface on the original plane[19]. This process can repeat on the cross slip plane so that the entire region near the original source becomes relaxed.

Heterogeneous sources of this type are limited, however, the result being that considerable relaxation can develop in areas near a source, with very little relaxation in other areas[5]. These mechanisms are also consistent with the observation that for small

mismatch strains, more than one dislocation is often observed on the same or close-by glide planes. Extensive TEM observations[18] suggest that no multiplication at intersections by the mechanism suggested by Hagen and Strunk[20] is required. This mechanism, although geometrically possible, requires a rather improbable series of events at an intersection between two dislocations of like Burgers vector. So far, *in-situ* confirmation of multiplication has not been observed, even after viewing a large number of such intersection reactions[21].

When the lattice mismatch reaches approximately 2%, the misfit stress is high enough to nucleate half-loops directly at the epilayer surface[22,23], diagrammed in Figure 9. Experimental observations of plan view TEM specimens have convincingly demonstrated this change in mechanism at 1.8% lattice mismatch[9,24]. For these larger mismatch cases, the configuration of misfit dislocations changes dramatically: instead of relatively long segments of 60° dislocation lying in the interface in a crossed grid, a much larger number of very short segments are generated whose Burgers vectors correspond to the two 1/2<011> dislocations which lie in the (100) interface plane (Figure 10). This has been interpreted as the onset of surface nucleation of half-loops[24], in part because the spatial distribution of nucleation sites increases dramatically and becomes more uniformly distributed within a small range of misfit near 2%. These sites may be steps or local compositional variations, or they may be surface roughness associated with an incipient transition to Stranksi-Krastanov (three-dimensional) growth.

This large number of sites greatly increases the probability of reactions between two 60° misfit dislocations to form a single edge-type misfit segment. A length of edge dislocation provides the same mismatch strain relief as the two 60° dislocations it replaces, while the total dislocation line energy is cut in half.

It is also probable that these reactions between 60° dislocations are not just by chance: if one 60° dislocation half-loop is nucleated and glides to the heterointerface, its stress field promotes the nucleation of the complementary 60° dislocation, having opposite

screw and surface-normal components. This makes it extremely likely that nucleation will usually occur as complementary pairs. The TEM observations show that very few unreacted 60° dislocations remain in the heterointerface under epilayers with $\geq 2\%$ mismatch (see Figure 10). Another natural consequence of the sudden dramatic increase in the density of nucleation sites above this mismatch is a sudden large increase in threading dislocation density, since each short segment of misfit dislocation is just part of a half-loop, both ends of which extend through the epilayer to the growth surface[25].

It is not yet clear whether or not most of these threading dislocations in the Ge_xSi_{1-x} epilayers at or above 2% mismatch are the unreacted arms of the original 60° dislocation half-loops, or if the reaction nodes, originally near the heterointerface, move into the cross slip planes to complete the reaction all the way to the surface, resulting in sessile edge threading segments. A few unreacted cases have been observed, but in most cases the epilayers have been too thin to determine the exact nature of these epithreading arms. (The inability to deconvolute the images of the epithreading arm and the misfit dislocation may, in fact, be taken as secondary evidence that the reaction has gone to completion.)

Whether or not they are reacted, the net Burgers vector taken over a large number of threading dislocations introduced by such a homogeneous mechanism would be expected to be zero. For each of the possible six Burgers vectors, there should be, within a few interdislocation distances, another dislocation with the same Burgers vector but opposite line direction. Interactions between threading dislocations (both attractive and repulsive) may also contribute to the shortness of individual dislocation segments, in part by stopping the glide of extending misfit half-loops.

Mechanisms for elimination of threading segments are of great interest for high mismatch epitaxial growth, particularly in the instance of GaAs/Si. Any growth conditions which can cause the bending of threading dislocations would be expected to increase the chance meeting of two arms of inverse sign (or otherwise attractive strain fields), thereby eliminating both (or at least one of the two) in the subsequent growth of the epilayer.

Thermal cycling, which would vary the magnitude (and, through differential thermal expansion, possibly even the sign) of mismatch stresses, would thus give dislocations greater chance to interact. Also, high temperature annealing, which increases both glide and climb mobilities, would be expected to promote annihilation or recombination reactions. Both these strategies have been shown to be effective in elimination of epithreading dislocations in GaAs layers on Si[26,27]. Figure 11 illustrates a technique which has been found to promote these combination and annihilation reactions by causing bending[28]. The alternating stresses within a strained layer superlattice have been shown to be effective in reducing epithreading densities to $\sim 10^8 cm^{-2}$. Rapid thermal annealing, where incresed thermally-activated glide mobility is combined with varying thermal stresses, has also been shown to be more effective than conventional furnace annealing[29].

Another very promising method for promoting these reactions and thereby decreasing dislocation density in the final stages of GaAs/Si growth has been demonstrated by Yamaguchi, et al.[30] Thermal cycling during interrupted OMCVD growth was successful in reducing the epithreading density to $\sim 10^6 cm^{-2}$. The greater reduction may have been due in part to the differential thermal expansion coefficients of GaAs and Si: during cycling, the layer may have been in either tension or compression (or, if always in compression, at least to widely varying levels), allowing the dislocations to have a higher probability of moving into reaction configurations -- in essence, increasing the "capture cross section" for the annihilation reactions.

A third strategy for decreasing dislocation density in an epilayer, particularly for low mismatch layers, is patterned growth[31] (Fitzgerald). Experiments have been performed using small dimension mesas, mostly for InGaAs/GaAs and GeSi/Si low-mismatch epilayer growth. For small mismatches, this technique limited the number of heterogeneous sources which could introduce dislocations, and also allowed the half-loops that generate misfit dislocations to glide across the entire width of the mesa, leaving no

epithreading dislocations. This technique has been remarkably successful, although its applications to device fabrication are yet untested.

Conclusions

1) For heteroepitaxial layers of small enough mismatch, $\leq 1.8\%$, stacking faults, microtwins, inversion boundaries, and even threading dislocations can effectively be eliminated for layers above critical thickness h_c by use of high-quality substrates, complete avoidance of any contamination of the growth surface, choice of favourable orientation and geometry, and by restricting the area of the layer by patterned growth.

2) For larger mismath ($\geq 1.8\%$), the mechanism of introduction of misfit dislocations changes, with a concommitant large increase in epithreading dislocation density. The achievement of low dislocation densities in layers above h_c, therefore, depends on strategies which promote attractive and anihilation reactions between threading dislocations during or after layer growth. Even for these high misfit cases, it seems likely that, by using a combination of several of these strategies, reproducible growth of more new device-quality heteroepitaxial layers will become possible.

Acknowledgement

This work was supported by the Director, Office of Energy Research, Office of Basic Energy Sciences, Materials Sciences Division of the U.S. Department of Energy under contract No. DE-AC03-76SF00098.

References

1. J.W. Matthews, *Phil. Mag.*, **13**, 1207 (1966)
2. J.H. van der Merwe, *J. Appl. Phys.*, **34**(1), 123 (1963)
3. J.W. Matthews, A.E. Blakeslee, and S. Mader, *Thin Solid Films*, **33**, 253 (1976)
4. J.W. Matthews and A.E. Blakeslee, *J. Cryst. Growth*, **27**,118 (1974)
5. C.G. Tuppen, C.J. Gibbings, and M. Hockly, *J. Cryst. Growth*, **94**, 392 (1989)
6. E. Kasper and H.-J. Herzog, *Thin Solid Films*, **44**, 357 (1977)
7. J.C. Bean, L.C. Feldman, A.T. Fiory, S. Nakahara, and I.K. Robinson, *J. Vac. Sci. Tech. A*, **2**, 436 (1984)
8. R. Hull, J.C. Bean, D.J. Werder, and R.E. Leibenguth, *Appl. Phys. Lett.*,**52**(19), 1605 (1988)
9. E.P. Kvam, D.J. Eaglesham, D.M. Maher, C.J. Humphreys, J.C. Bean, G.S. Green, and B.K. Tanner, MRS Symp. Proc. Vol. **104**, 623 (1988)
10. D.C. Houghton, D.D. Perovic, J.-M. Baribeau, and G.C. Weatherly, *J. Appl. Phys.*, **67**(4), 1850 (1990)
11. J.Y. Tsao, B.W. Dodson, S.Y. Picraux, and D.M. Cornelison, *Phys. Rev. Lett.*, **59**(21), 2445 (1987)
12. B.W. Dodson and J.Y. Tsao, *Appl. Phys. Lett.*, **51**(17), 1325 (1987)
13. B.W. Dodson, *Phys. Rev. B*, **38**, 12383 (1988)
14. R. Hull, J.C. Bean, and C. Buescher, *J. Appl. Phys.*, **66**(12), 5837 (1989)
15. I.J. Fritz, Appl. Phys. Lett., *Appl. Phys. Lett.*, **51**(14), 1080 (1987)
16. D.C. Houghton, C.J. Gibbings, C.G. Yuppen, M.H. Lyons, and M.A.G. Halliwell, *Appl. Phys. Lett.*, **56**(5), 460 (1990)
17. D.J. Eaglesham, D.M. Maher, E.P. Kvam, J.C. Bean, and C.J. Humphreys, *Phys. Rev. Lett.*, **62**(2), 187 (1989)
18. D.J. Eaglesham, E.P. Kvam, D.M. Maher, C.J. Humphreys, and J.C. Bean, *Phil. Mag. A*, **59**(5), 1059 (1989)

19. C.G. Tuppen, C.J. Gibbings, M. Hockly, and S.G. Roberts, *Appl. Phys. Lett.*, 56(1), **54** (1990)

20. W. Hagen and H. Strunk, *Appl. Phys.*, **17**, 85 (1978)

21. R. Hull, private communication

22. F.C. Frank, in "Symposium on Plastic Deformation of Crystalline Solids", Carnegie Institute of Technology, Pittsburgh, p. 89 (1950)

23. J.P. Hirth, in "Relation between Structure and Strength in Metals and Alloys", H.M.S.O., London, p. 218 (1963)

24. E.P. Kvam, D.M. Maher, and C.J. Humphreys, MRS Symp. Proc. Vol. **160**, in press

25. E.P. Kvam, submitted to *Phil. Mag. Lett.*

26. M.M. Al-Jassim, T. Nishioka, Y. Itoh, A. Yamamoto, and M. Yamaguchi, MRS Symp. Proc. Vol. **116**, 141 (1988)

27. H.L. Tsai and J.W. Lee, *Appl. Phys. Lett.*, **51**, 130 (1988)

28. S.L. Wright and H. Kroemer, *Appl. Phys. Lett.*, **37**, 210 (1980)

29. Z. Lillienthal-Weber, MRS Symp. Proc. Vol. **148**, 205 (1989)

30. M. Yamaguchi, A. Yamamoto, M. Tachikawa, Y. Itoh, and M. Suga, *Appl. Phys. Lett.*, **53**,2293 (1988)

31. E.A. Fitzgerald, *JOM*, **41**(4), 20 (1989)

Figure Captions

Figure 1.

Incompletely deoxidized Si substrate has caused polycrystalline region and multiple defects in the GaAs epilayer.

Figure 2.

Facetted inversion domain boundary (left) induced by loss of symmetry between Si substrate (Fd3m) and GaAs epilayer ($\bar{4}3m$).

Figure 3.

Cross sectional <110> view of typical as-grown GaAs/Si(001) structure; many dislocations, often partials with associated stacking faults, wend through the epilayer.

Figure 4.

Schematic diagram of fully coherent, strained epilayer: the smaller parameter upper layer has tetragonally distorted to match the in-plane lattice parameter of the lower (substrate) crystal.

Figure 5.

Schematic diagram of relaxed mismatched epilayer, with 60° dislocation (left) and edge dislocation (right) at the heterointerface (c.f. Figure 4).

Figure 6.

Plan view of crossed grid of misfit dislocations at Ge-Si/Si(001) heterointerface.

Figure 7.

Stability diagram (following Matthews, et alia[1,3,4]): above the curve, strain energy release by glissile misfit dislocation introduction is greater than the dislocation core energy addition. The van der Merwe criteria[2] yields a curve which is lower by a small multiple.

Figure 8.

Threading dislocation from substrate may glide through epilayer, leaving misfit dislocation at heterointerface. Motion is driven by mismatch-induced strss F1, restrained by line tension F2.

Figure 9.

Dislocation half-loop, at high mismatch, may nucleate at surface and glide to heterointerface, leaving misfit dislocation, which extends as end epithreading segments glide apart.

Figure 10.

Short misfit dislocation segments after the onset of surface nucleation in $Ge_{0.5}Si_{0.5}/Si(001)$; change in contrast with diffracting conditions illustrates the edge character of the dislocations (left: **g** = 220; right: **g** = 400).

Figure 11.

Radical reduction in threading dislocations in upper GaAs (compared to initial interface) caused by dislocation deflection in the strained layer superlattice.

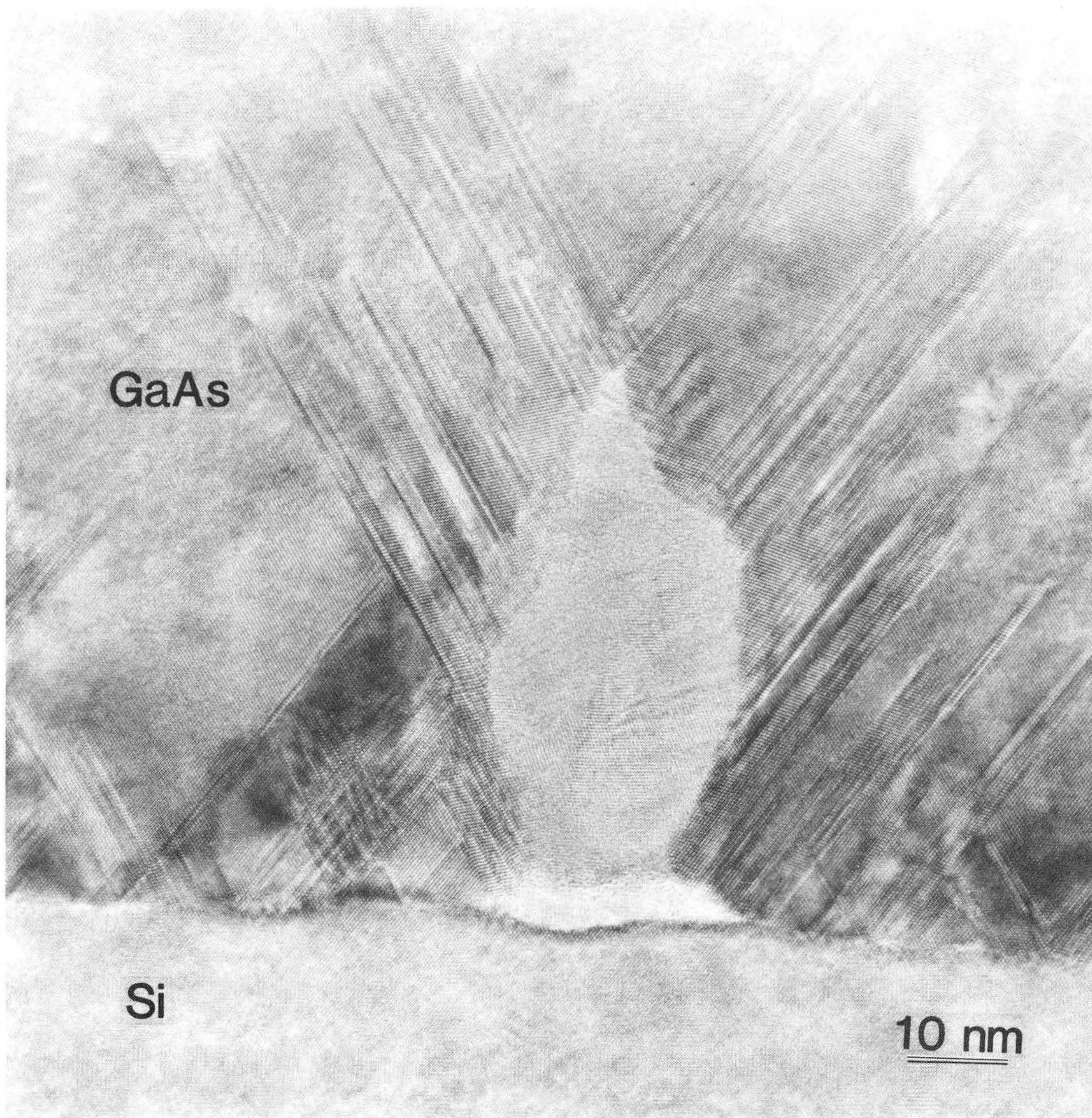

XBB 894-3155

Figure 1

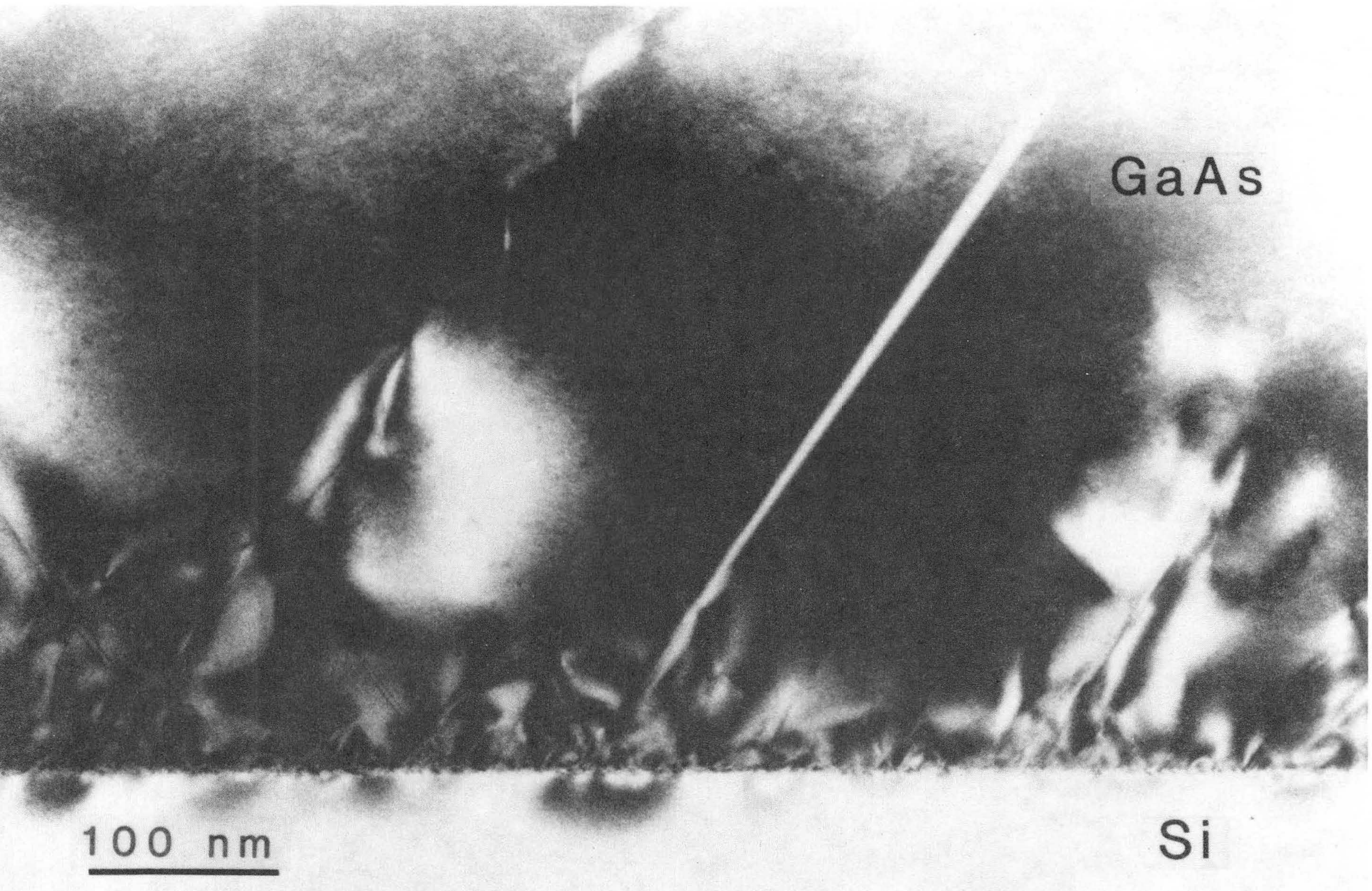

XBB 870-9410

Figure 2

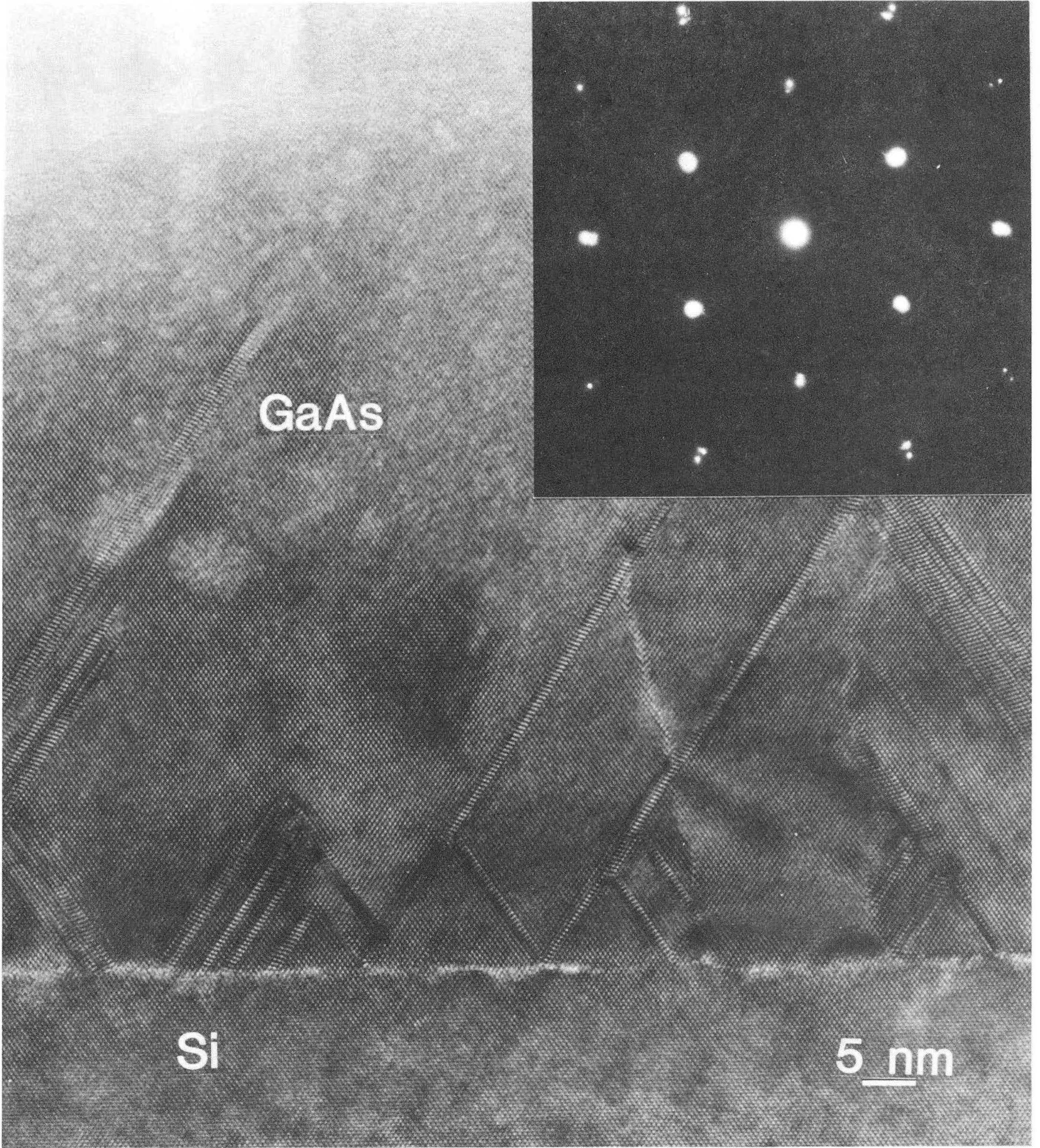

XBB 894-3152

Figure 3

XBL 903-981

Figure 4

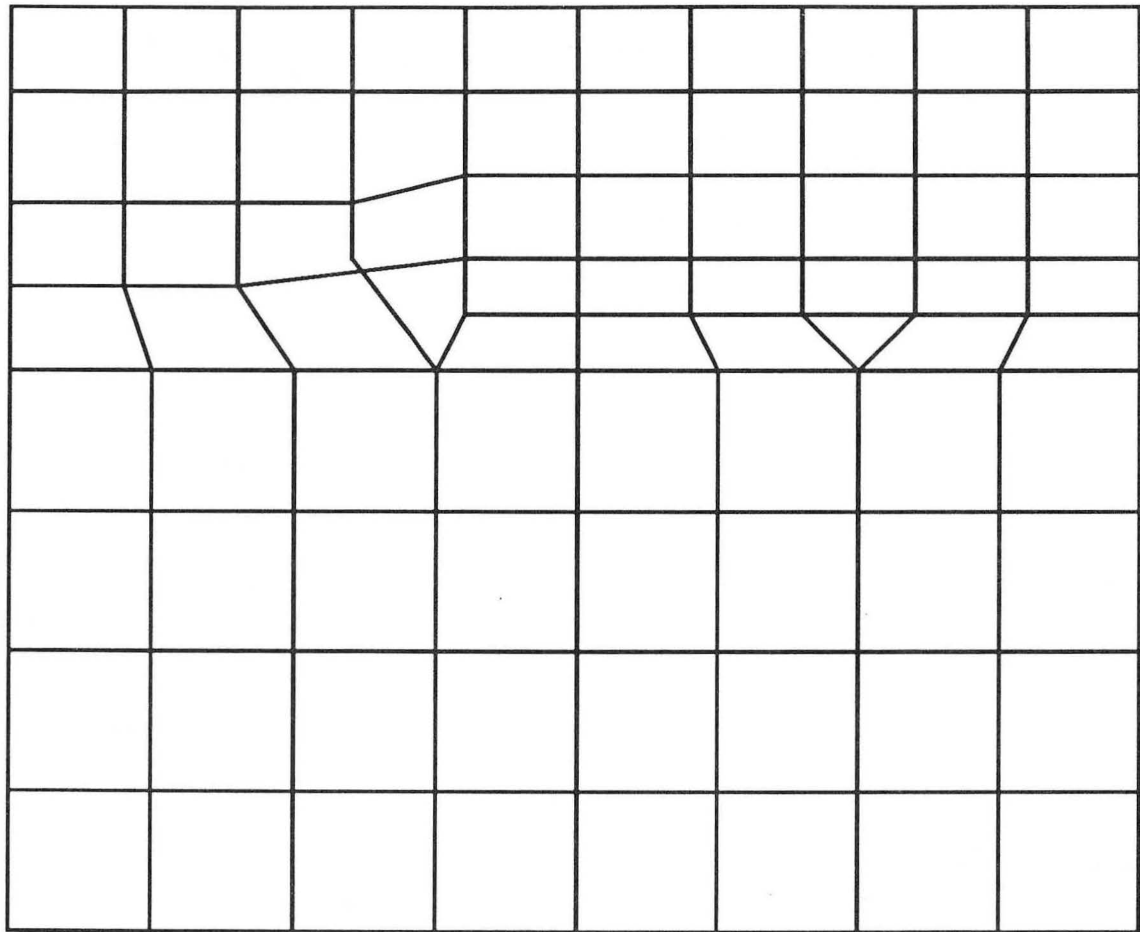

XBL 903-982

Figure 5

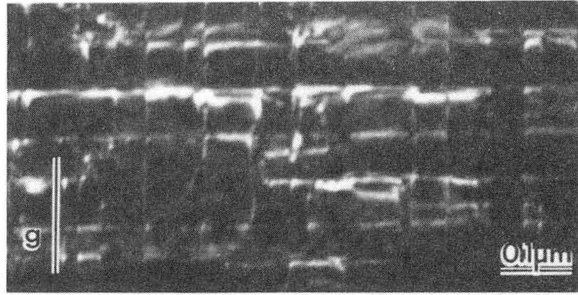

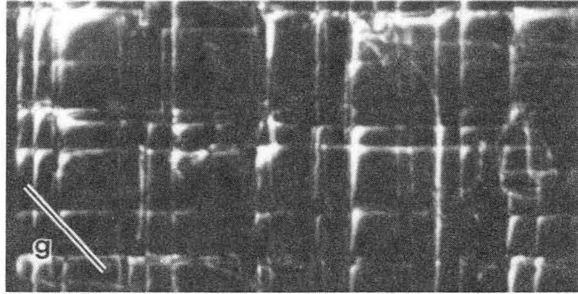

XBB 890-8782

Figure 6

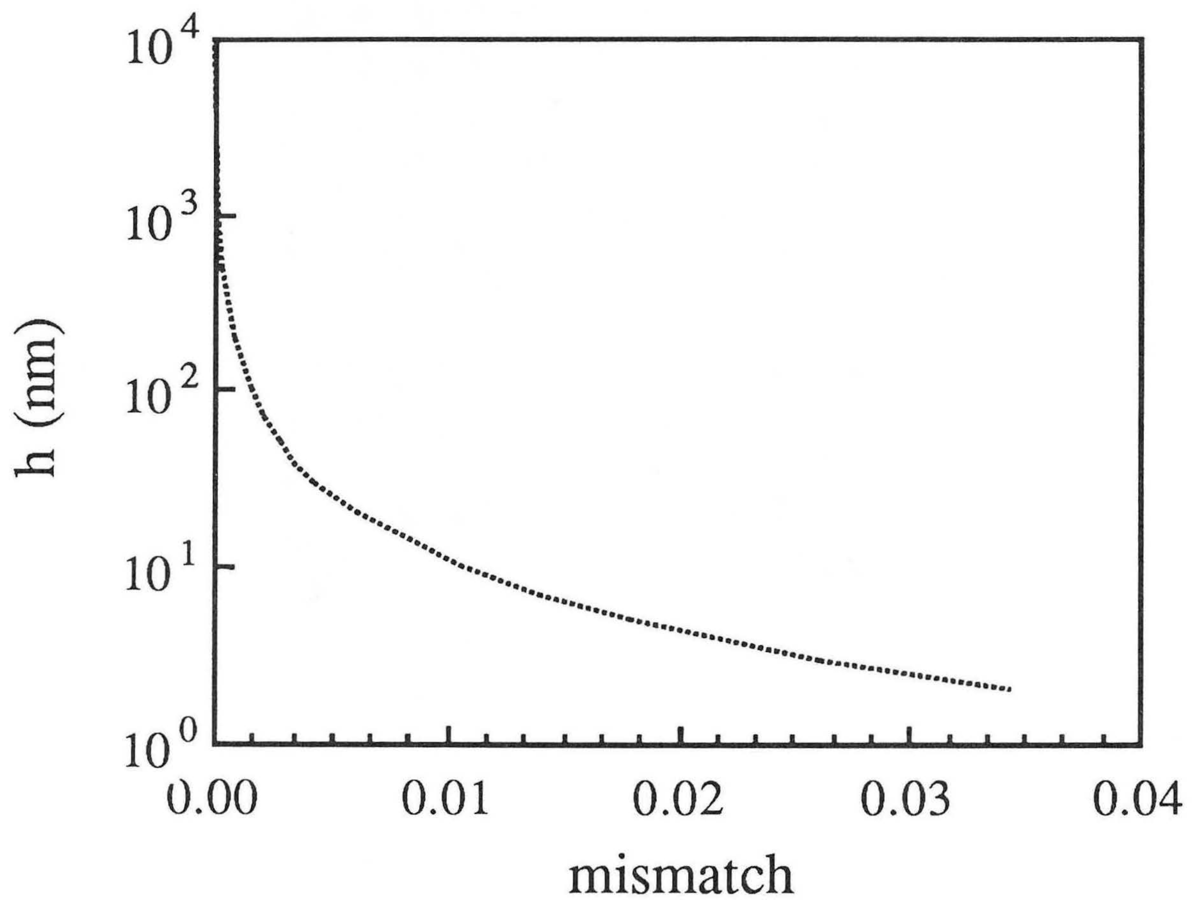

Figure 7

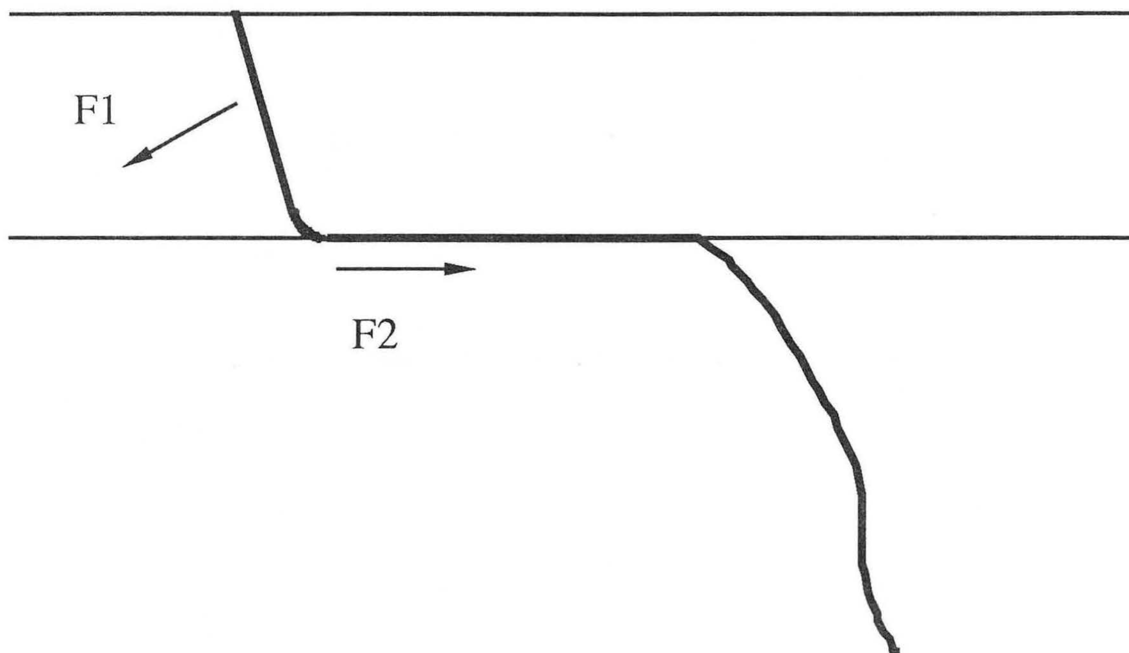

XBL 903-984

Figure 8

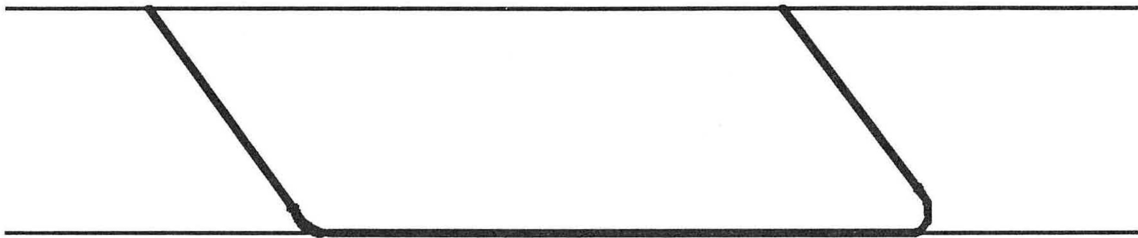

XBL 903-985

Figure 9

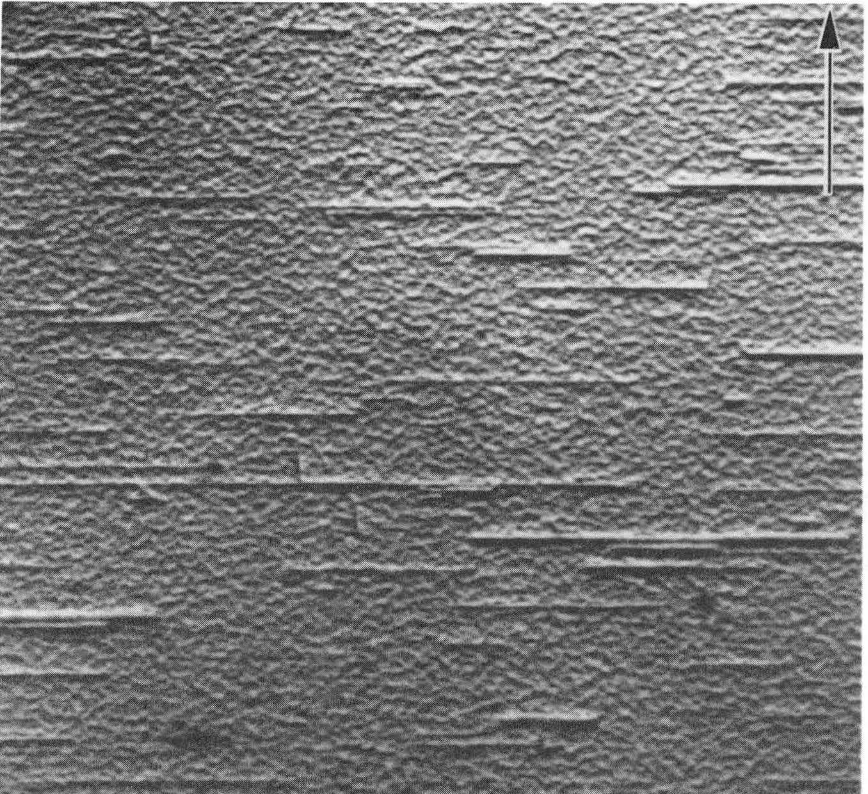

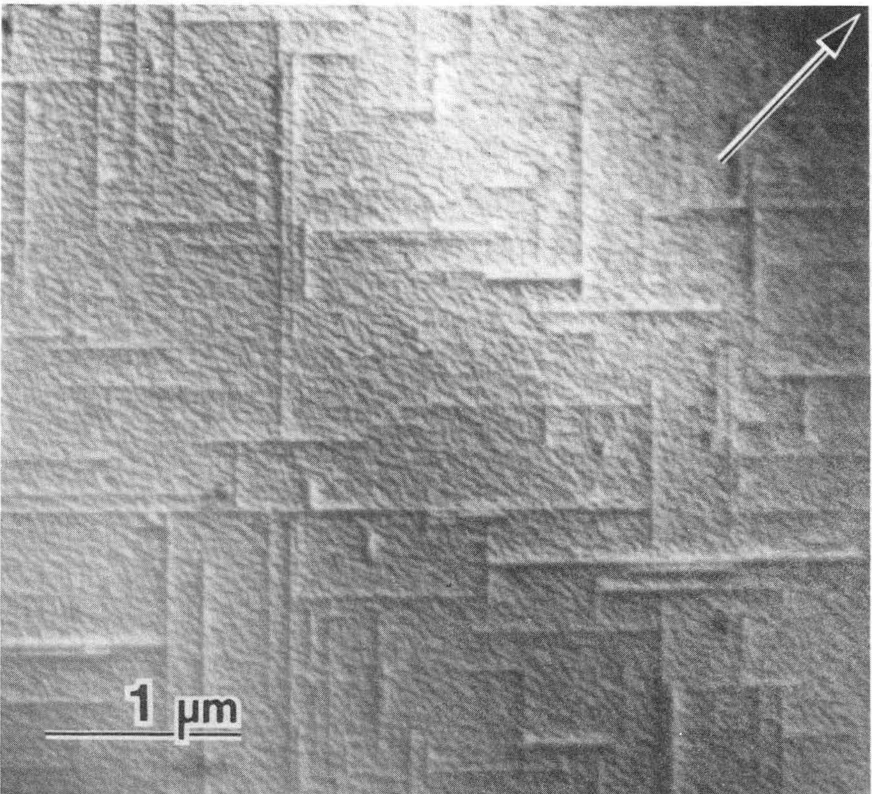

XBB 890-10459

Figure 10

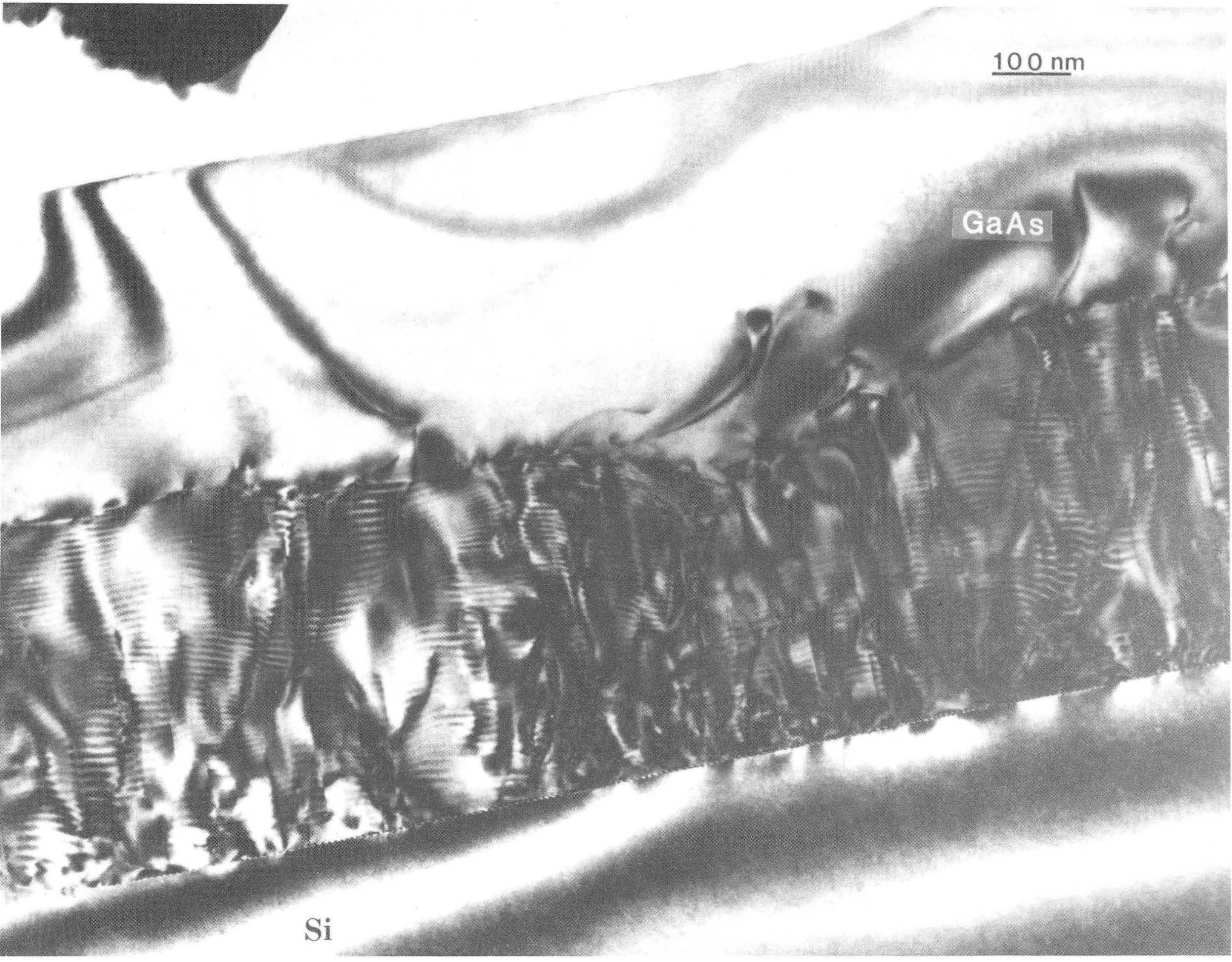

Figure 11

XBB 871-46

LAWRENCE BERKELEY LABORATORY
UNIVERSITY OF CALIFORNIA
INFORMATION RESOURCES DEPARTMENT
BERKELEY, CALIFORNIA 94720